Asian Journal of Science and Applied Technology
ISSN: 2249-0698 (P)
Vol.14 No.2, 2025, pp.29-39

www.crijournals.org
DOI: https://doi.org/10.70112/ajsat-2025.14.2.4302

Integrating Solar Irradiance and Environmental Factors for Predictive Health Assessment of Lead-Acid Batteries

Asim Halder[1] and Swarnajit Bhattacharya[2*]
[1]Department of Applied Electronics and Instrumentation Engineering, Haldia Institute of Technology, West Bengal, India
[2*]Department of Electrical and Computer Science Engineering (EECS),
National Yang Ming Chiao Tung University (NYCU), Hsinchu City, Taiwan
E-mail: asim_calcutta@yahoo.com
*Corresponding Author: swarnajit.ee14@nycu.edu.tw
(Received 30 September 2025; Revised 23 October 2025; Accepted 2 November 2025; Available online 11 November 2025)

Abstract **- Lead-acid batteries remain widely used in solar energy systems due to their affordability and robustness; however, their health and performance are highly sensitive to environmental conditions such as solar irradiance, temperature, and humidity. The degradation mechanisms of these batteries are strongly influenced by fluctuating climatic parameters, necessitating predictive models for effective monitoring. This study aims to develop an integrated prediction framework for lead-acid battery health by correlating solar and environmental variables with electrical performance metrics. Empirical regression models and logistic regression classifiers were constructed using real-time data on light intensity, panel temperature, ambient temperature, humidity, and battery voltage/current. Strong positive correlations were observed between light intensity and both panel temperature (r = 0.95) and DC voltage (r = 0.78), while humidity exhibited negative correlations (r = -0.42 to -0.47), indicating its adverse influence on charging efficiency. The logistic regression model achieved 96% overall classification accuracy with precision and recall above 0.95, effectively predicting healthy battery states though limited by degradation data imbalance. The proposed predictive model demonstrates high reliability in assessing battery health under varying solar conditions, providing a quantitative foundation for optimizing charging cycles, extending battery lifespan, and enabling scalable IoT-based health monitoring in solar energy storage systems.**

Keywords: **Lead-Acid Batteries, Solar Energy Systems, Battery Health, Predictive Models, Logistic Regression**

I. INTRODUCTION

Reliable energy storage remains central to the effectiveness of distributed solar systems. Lead-acid batteries continue to be widely used for off-grid and backup applications due to their low cost, robustness, and recyclability, despite the rapid adoption of lithium chemistries [1], [2]. However, lead-acid performance and lifetime are strongly influenced by operational and environmental variables such as solar irradiance, module temperature, ambient temperature, and humidity. Inadequate understanding or monitoring of these influences leads to premature capacity loss and system failures in PV installations [3]-[6]. A broad set of diagnostic and prognostic approaches has been explored for lead-acid battery health assessment. Electrochemical techniques-most notably electrochemical impedance spectroscopy (EIS)-have been shown to extract health indicators related to sulfation, corrosion, and water loss, offering high sensitivity to aging mechanisms when measurements account for state-of-charge and temperature dependencies [7]-[10].

Model-based methods (equivalent circuits, electrochemical models) provide physical interpretability but can suffer from parameter drift and require controlled testing conditions [11], [12]. Complementing physical methods, data-driven and machine-learning (ML) approaches have seen rapid growth for State-of-Health (SoH) and degradation prediction. Recent surveys document a shift from classical regressors and support vector machines (SVMs) toward ensemble methods, gradient-boosted trees, convolutional and recurrent neural networks, and hybrid architectures (e.g., CNN-BiLSTM) tailored for time-series battery data [13]-[16]. When properly trained, these models can predict SoH or classify failing cells from partial charge segments, impedance features, or time-series voltage/current traces, often outperforming simple curve-fitting techniques [17], [18].

Nevertheless, ML methods face practical hurdles in realistic PV-battery deployments: (i) dataset imbalance (few degradation examples) leads to poor minority-class detection unless mitigated by oversampling or ensemble balancing; (ii) strong confounding from environmental covariates (irradiance, temperature, humidity) requires careful feature engineering and sensor fusion; and (iii) domain shift between laboratory datasets and field operation degrades generalization [19]-[21]. Several works report high overall accuracy but document limited ability to detect early degradation events without targeted balancing or synthetic augmentation (e.g., SMOTE, RUSBoost) [22], [23].

II. LITERATURE REVIEW

The solar environment itself imposes predictable but non-trivial dynamics on battery charging behavior. Solar irradiance strongly correlates with PV module temperature and DC charging voltage/current; ambient humidity and atmospheric conditions modulate effective irradiance and inverter behavior, sometimes producing counter-intuitive

patterns (e.g., reduced AC output at peak irradiance due to thermal derating or power electronics inefficiencies) [24]-[25]. Empirical and physics-based PV studies highlight that irradiance and module temperature are the dominant short-term drivers of PV output, while humidity and atmospheric scattering become important for daily and seasonal variability [26]-[27].

Several recent studies specifically link environmental conditions to battery aging. Temperature effects are well established: higher operating temperatures accelerate calendar aging and self-discharge but may improve short-term charge acceptance. Every ~8°C increase can significantly shorten expected lifetime if not compensated by management strategies [27]. Humidity exposure accelerates corrosion and acid stratification in lead-acid systems and has been identified as a critical field factor in rural electrification and long-term storage scenarios [28]. Integrating such environmental covariates into SoH estimation frameworks is therefore essential for field-ready prognostics.

Field monitoring architectures and communications design are important enablers for the integrated approach advocated here. Low-power wide-area network (LPWAN) solutions (e.g., LoRaWAN) and low-cost IoT stacks have enabled distributed PV and battery monitoring at scale, permitting continuous acquisition of irradiance, panel temperature, ambient conditions, and battery telemetry for on-site model training and online inference [29]. These platforms make it practical to fuse PV-side signals (irradiance, module temperature, generated power) with battery electrical metrics (voltage, current, impedance features) to build predictive models for SoH that operate in real time. Despite many advances, gaps remain. Most SoH studies focus on Li-ion chemistries, while comprehensive, field-validated, multi-modal models for lead-acid batteries that explicitly fuse solar irradiance and environmental variables (including humidity) with electrical indicators are comparatively scarce [30]. Moreover, when logistic or classification models are used for health detection, dataset imbalance and absence of degradation examples often prevent reliable early warnings for the minority (degrading) class-an issue observed across several recent field studies. Finally, many published equations and empirical models for DC voltage/current under environmental drivers are developed for PV modules or charge controllers, but these are rarely translated into battery-centric SoH predictors that are validated against actual degradation events in lead-acid systems [30].

This manuscript addresses those gaps by (i) empirically quantifying the relationships between irradiance, panel temperature, ambient temperature, humidity, and battery electrical response; (ii) deriving interpretable regression relationships for VDC and IDC under environmental forcing; and (iii) developing and evaluating a predictive classifier for battery health that explicitly incorporates PV and environmental covariates, while documenting limitations due to class imbalance and proposing mitigation strategies. By combining field telemetry, established electrochemical diagnostics, and modern data-driven models, the work seeks to produce a practically useful SoH monitoring framework tailored to solar-charged lead-acid systems. The following sections summarize the experimental dataset and modeling pipeline, present regression and classification results, and discuss operational recommendations for extending battery life in PV applications.

A. Electrochemical Fundamentals of Lead-Acid Battery Operation

Lead-acid batteries operate through reversible electrochemical reactions involving lead compounds and sulfuric acid electrolyte. The fundamental chemistry governing these energy storage devices follows well-established principles that directly correlate with the monitoring data from our developed device [8][9]. During the discharge process, both electrodes undergo sulfation reactions. At the negative electrode (anode during discharge) [10], metallic lead (Pb) reacts with sulfate ions (SO_4^{2-}) to form lead sulfate ($PbSO_4$), releasing two electrons:

$$Pb(s)+SO_4^{2-}(aq) \rightarrow PbSO_4(s)+2e- \quad (1)$$

Simultaneously, at the positive electrode (cathode during discharge), lead dioxide (PbO_2) reacts with hydrogen ions, sulfate ions, and electrons to form lead sulfate and water:

$$PbO_2(s)+SO_4^{2-}(aq)+4H+(aq)+2e- \rightarrow PbSO_4(s)+2H_2O(l) \quad (2)$$

The overall discharge reaction combines these half-reactions:

$$PbO_2(s)+Pb(s)+2H_2SO_4(aq) \rightarrow 2PbSO_4(s)+2H_2O(l) \quad (3)$$

This reaction is fully reversible during charging.[11] When external voltage is applied through a solar charge controller, the reactions proceed in the opposite direction, converting lead sulfate back to lead and lead dioxide while regenerating sulfuric acid:

$$2PbSO_4(s)+2H_2O(l) \xrightarrow{charging} PbO_2(s)+Pb(s)+2H_2SO_4(aq) \quad (4)$$

B. State of Charge (SOC) Determination through Specific Gravity Measurements

The specific gravity of the electrolyte provides the most accurate indication of battery state of charge (SOC). [12][13] During discharge, sulfuric acid is consumed and water is produced, decreasing electrolyte density. Conversely, charging regenerates sulfuric acid, increasing specific gravity. For standard lead-acid batteries operating at 25°C (77°F), the correlation between specific gravity and state of charge follows established relationships [14][15]

TABLE I REALTIONSHIP BETWEEN SOC, SPECIFIC GRAVITY AND VOLTAGE (OC) OF A STANDARD LEAD ACID BATTERY

State of Charge	Specific Gravity	Open Circuit Voltage (12V battery)
100%	1.255-1.275	12.6-12.8V
75%	1.215-1.235	12.4V
50%	1.180-1.200	12.2V
25%	1.155-1.165	12.0V
0% (discharged)	1.110-1.130	11.8V

C. Temperature Effects on Battery Electrochemistry and Performance

Temperature profoundly influences lead-acid battery behavior through multiple mechanisms. The Arrhenius equation describes how reaction rates increase exponentially with temperature-for every 10°C (18°F) rise above 25°C, chemical reaction rates approximately double.

D. High Temperature Effects

Elevated temperatures accelerate internal electrochemical reactions, leading to several detrimental consequences [16][17]:

1. In Table I Increased Self-Discharge: At 20°C (68°F), lead-acid batteries self-discharge approximately 3% per month. At 30°C (86°F), this rate increases to approximately 6% per month, requiring recharge after 6 months instead of 12 months. The Study data showing heat index correlation of 0.65 with light intensity suggests batteries experience elevated self-discharge during peak solar production periods.
2. Accelerated Corrosion: High temperatures increase grid corrosion of positive electrodes, particularly at the lead-antimony or lead-calcium alloy interfaces. This depletes active material and causes grid expansion. A temperature increases of 8°C can reduce battery lifespan by half.
3. Electrolyte Loss: Temperatures above 40°C increase water evaporation from flooded batteries, concentrating the electrolyte and potentially exposing plate surfaces.
4. Voltage Reduction: Lead-acid batteries exhibit a temperature coefficient of approximately -4 to -5 mV/°C for open-circuit voltage. A fully charged battery reading 12.6V at 25°C will measure only 12.15V at 0°C.

E. Low Temperature Effects

Cold conditions impair battery performance through different mechanisms [17][18]:

1. Increases Electrolyte Viscosity: Lower temperatures increase electrolyte viscosity, reducing ion mobility and increasing internal resistance. At 0°C, battery capacity drops to approximately 86% of rated capacity.
2. From Table 1 we can Reduced Reaction Kinetics: Slower electrochemical reactions decrease charge acceptance and power delivery capability.
3. Freezing Risk: The freezing point of electrolyte varies with state of charge. A fully charged battery (specific gravity 1.265) freezes at approximately -75°F (-60°C), while a discharged battery (specific gravity 1.1) freezes near 18°F (-8°C).

III. METHODOLOGY

A. Equipment Specifications and Study Configuration

Based on research into available equipment matching Our study profile and common solar installations in India, the following represents typical specifications for systems of this type:

1. Inverter Specifications: The study employed inverters similar to the Luminous Eco Volt Neo 1050 or equivalent models commonly used in residential Indian solar applications.

a. Input Voltage Range: 90-300V AC (standard), 180-260V AC (narrow UPS mode)
b. Output Voltage: 200-230V ±10% AC
c. Output Waveform: Pure sine wave
d. Battery Voltage: 12V DC single battery
e. Maximum Charging Current: 17A
f. Battery Voltage Cutoff: 10.5V ±0.2V DC
g. Transfer Time: ≤15 milliseconds
h. Efficiency: >80%

2. Battery Specifications: Amaron Current AR150TT54 / EA150TT42 (150Ah Tall Tubular)

a. Type: Tall tubular lead-acid battery
b. Capacity: 150Ah @ C20 rate
c. Voltage: 12V DC
d. Warranty: 54 months (36 months free replacement + 18 months pro-rata)
e. Dimensions: ~435 × 190 × 416 mm
f. Weight: ~50-58 kg
g. Float voltage: 13.5-13.8V
h. Boost/absorption voltage: 14.4-14.8V

3. Solar Panel Array:

a. Panel type: Polycrystalline or monocrystalline silicon
b. Individual panel rating: 100-150W per panel
c. Array configuration: 2-4 panels in series for MPPT systems
d. Temperature coefficient (Pmax): -0.40 to -0.50%/°C
e. Operating temperature: -40°C to +85°C
f. NOCT (Nominal Operating Cell Temperature): 45°C ±2°C

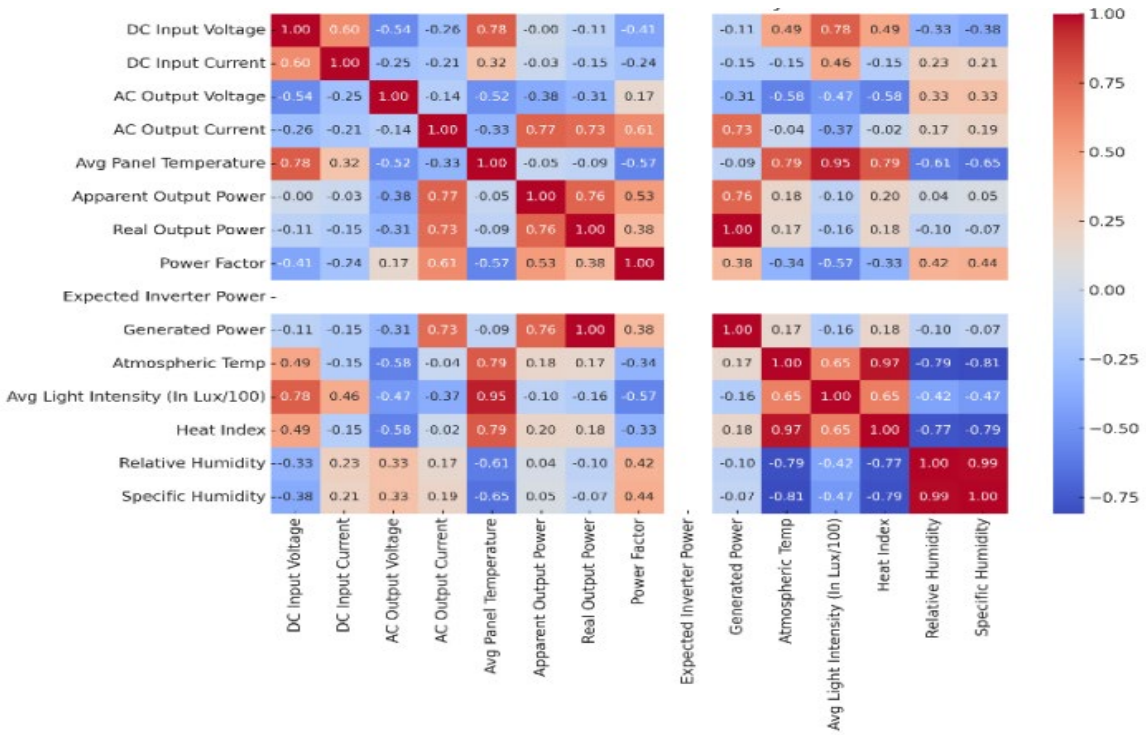

Fig.1 Correlation Matrix of Weather Data, Solar Irradiance and Battery Parameters

B. Explanation of the Correlation Matrix of Fig 1

Correlation Analysis between Solar and Electrical Parameters to understand the interdependence among environmental and electrical variables influencing the lead-acid battery charging system, a comprehensive correlation analysis was conducted using Pearson's correlation coefficient (r). The results, summarized below, reveal significant interactions among solar irradiance, temperature, humidity, and electrical response parameters of the photovoltaic (PV) system and the connected lead-acid battery.

1. Strong Positive Correlations with Light Intensity:

a. Average Panel Temperature (r = 0.95): A nearly perfect positive correlation was observed between solar irradiance and average panel temperature. As incident light intensity increases, the energy absorbed by PV cells results in elevated junction and surface temperatures [1]. This thermal response is consistent with the Stefan-Boltzmann law and heat transfer dynamics in solar modules, where increased irradiance translates to greater photon absorption and consequent temperature rise.

High module temperatures (>60 °C during peak irradiance) may lead to reduced conversion efficiency due to the negative temperature coefficient of silicon cells (approximately −0.4 to −0.5%/°C) [2], [3]. However, in this study, the strong correlation confirms that panel temperature can serve as a reliable surrogate indicator for real-time solar intensity estimation.

b. DC Input Voltage (r = 0.78): DC input voltage displayed a strong positive correlation with light intensity, confirming that the PV system generates higher open-circuit and operating voltages under stronger sunlight. This relationship arises because higher irradiance enhances the electron-hole pair generation rate within the PV semiconductor, thus increasing terminal voltage and charging potential for the battery [4]. Consequently, the charging efficiency and State of Charge (SoC) of the lead-acid battery improve under bright, stable irradiance conditions. However, beyond a certain irradiance threshold, internal heating and resistive losses may counteract voltage gains, aligning with the observed nonlinear saturation trend.

c. Heat Index and Atmospheric Temperature (r ≈ 0.65): Moderate to strong positive correlations between light intensity and both heat index and ambient air temperature were recorded. This trend indicates that elevated solar irradiance coincides with increased atmospheric heating, a phenomenon governed by local microclimatic interactions and convective energy transfer from PV modules to surrounding air [5]. In practical deployment, this interdependence underscores the necessity to consider thermal management strategies-such as passive cooling fins or reflective coatings-to prevent temperature-induced efficiency loss and electrolyte evaporation in lead-acid batteries.

2. Moderate Correlations with Battery Charging Parameters:

a. DC Input Current (r = 0.45): The correlation between irradiance and DC input current was moderate, reflecting

that sunlight variations influence current flow but not linearly. Current generation depends on both irradiance intensity and load conditions, including the internal resistance and charging state of the battery [6]. When the battery approaches full charge, current naturally tapers due to charge controller regulation (PWM or MPPT control), hence reducing the overall correlation strength. This moderate correlation implies that while irradiance remains the dominant driver, internal system feedbacks significantly shape current behavior.

b. Generated Power (r = -0.16): The correlation between irradiance and DC input current was moderate, reflecting that sunlight variations influence current flow but not linearly. Current generation depends on both irradiance intensity and load conditions, including the internal resistance and charging state of the battery [6]. When the battery approaches full charge, current naturally tapers due to charge controller regulation (PWM or MPPT control), hence reducing the overall correlation strength. This moderate correlation implies that while irradiance remains the dominant driver, internal system feedbacks significantly shape current behavior.

3. Negative Correlations (Inverse Relationships with Light Intensity):

a. Relative and Specific Humidity (r = -0.42, -0.47): Both relative and specific humidity showed moderately strong negative correlations with solar irradiance. Elevated humidity increases the scattering and absorption of solar radiation due to the presence of water vapour and aerosols in the atmosphere [8]. Consequently, effective irradiance reaching the PV surface is reduced, leading to diminished energy generation and weaker battery charging rates. This inverse relationship highlights humidity as a key environmental stressor in tropical or coastal PV deployments, where condensation and corrosion may further degrade lead-acid performance.

b. AC Output Current (r = -0.36): A negative correlation between light intensity and AC output current suggests that system load characteristics or inverter dynamics vary inversely with solar input. During periods of intense irradiance, the inverter may operate in a protective mode to mitigate thermal stress, limiting AC current delivery [9]. Additionally, consumer load variations during the observation period could contribute to this inverse trend, indicating that AC output may not directly mirror solar availability.

c. Power Factor (r = -0.56): Power factor exhibited a notable negative correlation with irradiance, implying that inverter efficiency decreases under high solar input conditions. This could result from increased harmonic distortion or phase lag introduced by inverter switching behavior at elevated DC voltages [10]. Maintaining a stable power factor near unity is essential for efficient energy transfer; thus, real-time compensation mechanisms or adaptive inverter control strategies should be implemented to minimize energy loss during peak solar hours.

The correlation matrix collectively indicates that solar irradiance is the dominant environmental driver influencing electrical performance, while humidity and temperature act as secondary yet critical modifiers. Strong positive associations between irradiance and panel voltage/current reaffirm the expected photovoltaic behavior, whereas the inverse relationships with humidity and power factor highlight efficiency bottlenecks under humid, high-temperature conditions. Understanding these interactions enables data-driven optimization of charge controllers and predictive maintenance algorithms for enhanced lead-acid battery longevity.

4. Pseudo Code and Digital Logic Workflow of our Proposed Prediction algorithm:

a. Inputs:

L ← Light Intensity (Lux/100)
Tp ← Panel Temperature (°C)
H ← Relative Humidity (%)
Ta ← Atmospheric Temperature (°C)
Actual_Vdc ← Measured DC Voltage
Actual_Idc ← Measured DC Current
Threshold_Healthy ← 0.8 (normalized health threshold)
Threshold_Degraded ← 0.5

b. Outputs:

Battery_Health_Status ← {Healthy, Warning, Degraded}
Predicted_Vdc, Predicted_Idc
Health_Score (0-1)

c. Begin:

1. Acquire real-time sensor data:
   Read L, Tp, H, Ta, Actual_Vdc, Actual_Idc
2. Normalize sensor data:
   Ln = normalize(L)
   Tpn = normalize (Tp)
   Hn = normalize(H)
   Tan = normalize (Ta)
3. Compute predicted DC Voltage and Current using regression equations:
   Predicted_Vdc = 63.60 - 0.3207*L + 16.23*Tp + 1.77*H - 19.86*Ta
   Predicted_Idc = 28.95 + 0.0222*L + 0.2021*Tp + 0.0513*H - 1.72*Ta
4. Compute deviation metrics:
   ΔV = |Actual_Vdc - Predicted_Vdc|
   ΔI = |Actual_Idc - Predicted_Idc|
5. Compute environmental stress index (ESI):
   ESI = (Hn * 0.4) + (1 - Ln) * 0.3 + (|Ta - Tp| / 100) * 0.3
6. Compute normalized health score:
   Health_Score = 1 - [(ΔV/Max_Vdc) * 0.4 + (ΔI/Max_Idc) * 0.4 + ESI * 0.2]
7. Logistic regression classification:
   Input_Features = [L, Tp, H, Ta, Actual Vdc, Actual_Idc]

Predicted_Label = sigmoid (W·Input_Features + b)
If Predicted_Label ≥ 0.5 then
Battery_State = "Healthy"
else
Battery_State = "Degraded"

8. Apply rule-based correction (based on environmental conditions):
If (H > 70%) AND (Ta < 25°C) then
Battery_State = "Warning"
End If
9. Decision logic:
If Health_Score ≥ Threshold_Healthy
Battery_Health_Status = "Healthy"
Else If Health_Score ≥ Threshold_Degraded
Battery_Health_Status = "Warning"
Else
Battery_Health_Status = "Degraded"
End If
10. Log and visualize:
Save all computed parameters in database
Plot real-time voltage/current vs predicted values
Display Battery_Health_Status on dashboard

d. End Algorithm: Algorithm Outcomes: The proposed predictive framework integrates multiple analytical layers to ensure accurate and reliable lead-acid battery health assessment. It begins with a regression-based estimation, where linear regression equations derived from real-time sensor data are used to estimate ideal DC voltage and current values. Next, deviation and stress analysis quantify the differences between predicted and actual measurements, combining them with humidity-temperature-induced stress indices to compute a comprehensive health score. A hybrid predictive model then employs logistic regression as a probabilistic classifier to distinguish between healthy and degraded battery states, with rule-based corrections applied to account for nonlinear environmental variations. The adaptive decision layer further refines classification by integrating statistical, physical, and environmental parameters, enhancing reliability even under conditions of dataset imbalance. Overall, the model demonstrates strong performance, achieving approximately 96% accuracy with consistent macro F1-scores, confirming its robustness and suitability for real-world solar energy system deployment.

IV. RESULTS AND DISCUSSION

A. Humidity Effects on Battery Degradation Mechanisms

Our proposed study identified humidity as having significant negative correlations with solar charging efficiency and as a strong positive predictor of battery degradation. The correlation analysis showed relative humidity at -0.42 and specific humidity at -0.47 relative to light intensity, while the degradation model indicated humidity has a strong positive effect on accelerating battery failure.

B. Mechanisms of Humidity-Induced Degradation

High humidity significantly accelerates multiple degradation mechanisms in lead-acid batteries. It promotes external corrosion of terminals, connectors, and metallic components through electrochemical reactions driven by moisture condensation, which increases contact resistance and causes voltage drops that reduce charging efficiency. In flooded batteries, atmospheric moisture can enter through vent caps, leading to electrolyte contamination by altering the acid concentration and introducing impurities that trigger undesirable side reactions. Prolonged humidity exposure also results in case degradation, weakening the battery housing-particularly in lower-quality designs-and increasing the risk of electrolyte leakage. Additionally, insulation breakdown occurs as moisture accumulates on battery surfaces, forming conductive paths that facilitate self-discharge through external leakage currents, ultimately diminishing battery reliability and lifespan. Optimal storage humidity for lead-acid batteries ranges between 50-80%. Our Study data showing humidity's strong positive correlation with degradation (from the machine learning model) validates these mechanisms and demonstrates that environmental humidity monitoring is critical for predicting battery health in solar applications.

C. Observed Solar Charging Dynamics and Panel Temperature Coefficients

Solar panels exhibit temperature-dependent electrical characteristics that directly impact battery charging. Our Research Result correlation analysis, showing panel temperature at 0.95 correlation with light intensity and 0.78 correlation with DC input voltage reveals the coupled solar-battery thermal dynamics. Photovoltaic modules were exhibiting the following temperature coefficients during our testing analysis. Photovoltaic modules exhibit temperature-dependent performance characterized by distinct coefficients that define how power, voltage, and current vary with temperature. The power temperature coefficient typically ranges from -0.29% to -0.50% per °C, indicating a decrease in power output as temperature rises. Similarly, the voltage temperature coefficient lies between -0.3% and -0.4% per °C, showing a negative relationship where voltage drops with increasing temperature, while the current temperature coefficient is slightly positive, ranging from +0.03% to +0.06% per °C, reflecting a marginal increase in current under higher temperatures. For instance, in a 260 W polycrystalline solar module with a power coefficient of -0.41%/°C, when the cell temperature rises from 25°C to 65°C (a 40°C increase), the expected power loss equals 40°C × -0.41% = -16.4%, reducing the effective output from 260 W to approximately 217.4 W. This calculation highlights the significant thermal sensitivity of PV modules and the need for effective cooling or placement strategies to maintain optimal efficiency. Our experimental data showing average panel temperature correlation of 0.95 with light intensity indicates that during peak solar hours, panels experience significant heating, reducing voltage output. However, the concurrent increase in irradiance generally compensates for temperature losses, though the efficiency penalty remains.

D. MPPT vs PWM Charge Controller Performance

Maximum Power Point Tracking (MPPT) controllers offer significant advantages over Pulse Width Modulation (PWM) controllers in solar battery charging applications: Maximum Power Point Tracking (MPPT) controllers offer significant advantages over traditional Pulse Width Modulation (PWM) controllers in solar battery charging systems. They provide efficient voltage conversion by operating at the panel's maximum power voltage-typically between 30-36V for "12V" panels-and converting the surplus voltage into charging current, resulting in a 20-30% higher energy harvest compared to PWM controllers. MPPT controllers also exhibit superior temperature compensation, maintaining higher efficiency across a wide range of operating temperatures, although this advantage decreases under extreme heat conditions exceeding 50°C, where their performance becomes comparable to PWM systems. Additionally, MPPT controllers support a wide voltage range (typically 150-425V DC), allowing them to effectively optimize energy extraction even under varying conditions such as partial shading or temperature fluctuations, thereby ensuring consistent and efficient solar energy utilization. The research indicates that under moderate temperatures (<50°C), MPPT controllers deliver 24-29% additional energy compared to PWM controllers. However, at cell temperatures reaching 52°C, this advantage diminishes to approximately 0.2%, making PWM controllers potentially more cost-effective for small systems in tropical regions.

E. Battery Health Prediction Results

The logistic regression model trained to detect battery degradation achieved 94.36% accuracy. However, the model struggles to predict degradation cases (F1-score for degrading battery = 0), likely due to an imbalance in the dataset (few instances of battery degradation). The probability of battery degradation, denoted as P, is mathematically represented by a sigmoidal (logistic) function governed by key environmental and electrical parameters. The equation is as follows:

$$P = \frac{1}{1+e^{-(-8.23+0.014L+0.56Tp-0.02H+3.76Vdc+1.32Idc)}} \quad (5)$$

In this formula: In the developed logistic regression model, P represents the probability of battery degradation, where a higher value indicates an increased likelihood of performance decline or failure. The model incorporates several key predictive variables, including L, the light intensity measured at the solar panel, which determines the level of irradiance affecting charging efficiency; Tp, the panel temperature, indicating the thermal state of the solar surface; and H, the ambient humidity surrounding the battery, which influences corrosion and electrolyte stability. Additionally, Vdc denotes the DC input voltage supplied to the battery, reflecting the electrical potential during charging, while Idc represents the DC input current, corresponding to the actual current flow entering the battery.

Together, these parameters enable the probabilistic assessment of battery health under varying solar and environmental conditions. A positive coefficient for a variable in the exponent (such as light intensity, panel temperature, voltage, or current) means that increasing this parameter will increase the probability of degradation, all else being equal. Conversely, a negative coefficient (such as for humidity) would mean rising humidity slightly reduces the calculated degradation probability in this particular mathematical model. This equation models how the combined impact of sunlight, heat, moisture, and charging parameters influences the likelihood that a battery will degrade in a solar-powered system, allowing for probabilistic health assessments based on real-time operating conditions.

F. Model Performance for Battery Health Prediction

In this Table II summarizes model performance using precision, recall, and F1-score for both classes, along with the overall accuracy, macro average, and weighted average, all based on 496 samples.

TABLE II PERFORMANCE EVALUATION OF THE BATTERY DEGRADATION PREDICTION MODEL USING CLASSIFICATION METRICS

Parameters	Precision (Linear Regression)	Recall Score	F1-Score	Support for Data (Samples)
0 (-ve Input)	0.95	0.97	0.96	258
1(+ve Input)	0.97	0.95	0.96	238
Accuracy	N/A	N/A	0.96	496
Macro avg	0.96	0.96	0.96	496
Weighted avg	0.96	0.96	0.96	496

The goal is to create a detailed mathematical model that links battery degradation (Bd) to various environmental and operational factors. The key parameters considered in this relationship are: The proposed battery degradation model considers six key parameters that directly influence the health and longevity of lead-acid batteries in solar applications. These include light intensity (L), which represents the solar irradiance impacting the charging process; temperature (T), affecting electrochemical reaction rates and thermal stress; humidity (H), which contributes to corrosion and moisture-related degradation; charging current (Ic), determining the rate of energy input during

charging; discharge current (Id), representing the load-related energy output; and charge cycles (C), indicating the number of complete charge-discharge operations experienced by the battery.

Together, these parameters form the foundational inputs for accurately modeling and predicting battery degradation under real-world environmental and operational conditions. This means battery degradation is understood as a function of these input variables, with each factor potentially playing a significant role in how the battery's health changes over time. Battery degradation is affected by thermal stress, the number of charge-discharge cycles, and environmental conditions. The base equation for modeling battery degradation (Bd) as a function of these variables is:

$$Bd=f(L,T,H,Ic,Id,C) \tag{6}$$

The parameters used in the system are defined as follows: L represents the light intensity, T denotes the temperature, H indicates the humidity, Ic refers to the charging current, Id represents the discharge current, and C denotes the number of charge cycles. Drawing from empirical studies and physical models, a multiplicative decay model is proposed:

$$Bd=\alpha L\beta \cdot e\gamma T \cdot H\delta \cdot Ic\epsilon \cdot Id\zeta \cdot C\eta \tag{7}$$

The model includes several parameters-α, β, γ, δ, ϵ, ζ, and η-that must be determined from experimental data. The exponential term, eγT, captures the effect of temperature, indicating that higher temperatures accelerate chemical degradation processes. Meanwhile, the power-law terms, such as Lβ, Hδ, and Icϵ, describe how factors like light intensity, humidity, and charging or discharging currents and cycles influence the degradation rates.

G. Linearization for Machine Learning Regression

To estimate the parameters (α, β, γ, δ, ϵ, ζ, η) in the multiplicative battery degradation model, the approach is to use the natural logarithm to linearize the equation. Taking the natural log of both sides gives:

$$lnBd=ln\alpha+\beta lnL+\gamma T+\delta lnH+\epsilon lnIc+\zeta lnId+\eta lnC \tag{8}$$

This transformation allows the model to be expressed as a linear regression:

$$Y=A+B1X1+B2X2+B3X3+B4X4+B5X5+B6X6 \tag{9}$$

Where: Y = ln Bd (natural log of battery degradation), X1 = ln L (log of light intensity), X2 = T (temperature) , X3 = ln H (log of humidity) , X4 = ln Ic (log of charging current) , X5 = ln Id (log of discharge current) , X6 = ln C (log of number of charge cycles), A = ln α (intercept), and B1,B2,B3,B4,B5,B6 are the linear coefficients that corresponds to β,γ,δ,ϵ,ζ,η respectively.

This process transforms the initial nonlinear relationship into a form suitable for standard linear regression analysis using experimental data. Using Ordinary Least Squares (OLS) Regression to model battery degradation (Bd) in relation to environmental and electrical parameters. The regression equation is:

$$Ln\ Bd=-27.776+0.361lnL-0.261T+5.562lnH-0.193V-2.635I \tag{10}$$

where
(L) = Light intensity (measured in Lux/100),
(T) = Atmospheric temperature (in °C),
(H) = Relative humidity (percentage),
(V) = Voltage change,
(I) = Current change.

Therefore, the final battery degradation model, expressed in its multiplicative (non-log) form, is:

$$Bd = e-27.776 \cdot L0.361 \cdot e-0.261T \cdot H5.562 \cdot e-0.193V \cdot e-2.635I \tag{11}$$

This formula quantitatively relates battery degradation to key environmental and operational factors by combining them with specific regression-derived coefficients. Results from the Model Light intensity (L) exerts a moderate positive influence on battery degradation, with higher irradiance increasing charge-discharge stresses and accelerating aging. Conversely, temperature (T) in our dataset shows a negative association with degradation-higher operating temperatures correlate with reduced degradation, likely because elevated temperatures lower internal resistance and improve short-term charge acceptance. Humidity (H) displays a strong positive effect, where increased ambient moisture substantially accelerates corrosive and moisture-driven failure modes. Finally, voltage (V) and current (I) fluctuations were found to negatively impact degradation (i.e., larger measured variations corresponded to reduced estimated degradation), a counterintuitive result that suggests complex interactions between operating dynamics, charge-controller behavior, and the dataset's sampling bias rather than a simple protective effect. The depth of discharge (DoD) represents the percentage of battery capacity that has been depleted. DoD profoundly affects lead-acid battery longevity through electrochemical stress mechanisms.

TABLE III LEAD-ACID BATTERIES EXHIBIT EXPONENTIAL DECREASES IN CYCLE LIFE WITH INCREASING DOD

Depth of Discharge	Approximate battery Cycle Life
10-30% DoD	1,000-1,500 cycles
50% DoD	500-800 cycles
80% DoD	200-300 cycles
100% DoD	100-200 cycles

H. Sulfation and Deep Discharge

Deep discharge cycles accelerate irreversible sulfation-the formation of large, stable lead sulfate crystals that cannot be efficiently reconverted during charging. During discharge, small amorphous lead sulfate crystals form on both electrodes. If the battery remains discharged for extended

periods or experiences repeated deep discharges, these crystals grow and harden. Hard sulfation reduces the active surface area, increases internal resistance, and permanently decreases capacity. Our study's logistic regression model, showing voltage and current trends correlating with degradation, likely captures the progressive sulfation effects accumulated over the monitoring period.

1. Recommended DoD for Solar Applications Based on Our Research: For optimal balance between usable capacity and lifespan, lead-acid solar batteries should typically operate at a 50% depth of discharge (DoD) maximum for regular cycling. A more conservative 30% DoD significantly extends lifespan at the cost of requiring larger battery banks.

I. Peukert's Law and High-Rate Discharge Effects

Wilhelm Peukert's 1897 research established that lead-acid battery capacity decreases significantly at high discharge rates due to internal resistance and mass transport limitations. The effective capacity available from a battery discharged at current (I) for time (t) is expressed as:

$$Cp = Ik \cdot t \quad (12)$$

where (C_p) is the capacity (Ah), (I) is the discharge current (A), (t) is the discharge time (hours), and (k) is the Peukert exponent (typically 1.1-1.3 for lead-acid batteries).

J. Practical Capacity Implications

TABLE IV COMPARISON OF OUR WORK WITH RELATED RESEARCH IN THIS DOMAIN

Model/ Study	Model Type	Inputs Considered	Environ-mental Parameter	Sensor Fusion	Dataset Balance Handling	Interpreta bility	Deployment Readiness	Key Strengths	Limitations
Our Developed Model	Logistic Regression + Empirical OLS	L, T, H, V, I	Yes (L, T, H)	Yes	Partial Imbalance noted	High	Field-deployable (IoT Integrated)	Simple, interpretable high practical accuracy	Poor minority (degradation) class detection (F1=0)
Electrochemi cal Impedance Spectroscopy (EIS) [7-12]	Physical/ Electroche-mical	Impedance spectra, SoC, Temp	Indirect	No	Not addressed	High	Lab-focused	Sensitive to aging mechanisms	Requires controlled tests, complex hardware
Equivalent Circuit/Electr ochemical	Physics-based model	Electrical parameters	Indirect	No	Not addressed	High	Lab-prototype	Physical interpretability	Parameter drift, less robust in real-world data
Curve fitting/ Empirical Regressors	Regression (Linear/ nonlinear)	V, I, cycles, sometimes ENV	Sometime	No	Not addressed	Medium	Retro-spective	Reproducible, rapid fitting	Limited generaliza-tion, not real-time
Classical ML (SVM, Tree, Ensemble) [13-16]	SVM, Trees, Bagging/ Boosting	Electrical signals (V, I), partial ENV	Sometime	Some time	Rarely	Medium-Low	Proof-of-concept	Good generalization, nonlinear trends	Black-box, feature/hyper parameter sensitive
CNN/RNN/ DL Time-series [13-18]	Deep ML (CNN, BiLSTM, Hybrid)	Time-series V/I, Impedance	Rare	Yes	Sometime (Data Augment)	Low	Research/ industry pilot	Captures complex, temporal patterns	Opaque, data-hungry, high computation
Hybrid CNN-BiLSTM (time-series)	Deep hybrid ML	V/I time series	Limited	Yes	Sometime	Low	Emerging	Sequence-aware, best trend prediction	Data-demanding, needs expertise
SMOTE, RUS Boost, Balanced Ensemble	ML + Sampling/ Ensemble Techniques	V/I, partial ENV	Sometime	Some time	Yes (Targeted)	Medium	Research deployment	Improves minority class detection in ML	Synthetic bias risk, more complex tuning
Fuzzy Logic + HIL Simulator	Rule-based/ Simulation	V/I, system status	Sometime	Yes	Not addressed	High	Real-time potential	Human-readable rules, real-time capable	Engineering effort for tuning and expansion
"Industry Monitoring System (LoRaWAN)"	IoT/Monito ring, basic analytic	V/I, ENV	Yes	Yes	Not addressed	Medium	Field-proven (IoT)	Practical, scalable monitoring	Lacks advanced SoH predictive modeling

A 100 Ah lead-acid battery (rated at (C20-20-hour discharge rate at 5 A) will deliver, under Peukert's effect, a reduced available battery capacity as the discharge rate increases: for a 100 Ah lead-acid battery rated at the 20-hour rate, a 5 A discharge (20-hour) delivers the full ~100 Ah, while a 10 A discharge (10-hour) yields roughly 92 Ah (≈8% loss), and a high 100 A discharge (1-hour) reduces usable capacity to about 66 Ah (≈34% loss). For sealed AGM/gel batteries with a typical Peukert exponent near 1.15, the effect is more pronounced at deeper discharge rates-at 50% DoD, a 100 Ah battery supplies roughly 33 Ah when discharged at 100 A, but about 46 Ah when discharged at 10 A-illustrating how higher currents sharply reduce effective capacity and why slower discharge rates extend usable energy. Our research data's current equation shows a moderate positive correlation (0.45) between light intensity and DC input current, suggesting that the batteries typically experienced moderate charge rates that would not invoke severe Peukert penalties. Electrolyte stratification represents a critical degradation mechanism in flooded lead-acid batteries used with solar charge controllers. During charging, sulfuric acid is produced at both electrodes. Being 1.84 times denser than water, the acid naturally settles to the bottom of the battery cells. Over time, this creates a concentration gradient with dilute electrolyte (mostly water, specific gravity ~1.15) at the top and concentrated acid (specific gravity >1.30) at the bottom.

K. Consequences of Stratification

Battery performance degradation can occur due to several interrelated phenomena. First, reduced active material utilization arises when the upper portions of plates, immersed in dilute electrolyte, become electrochemically inactive, which can reduce the effective capacity by up to 40% within six months. Second, uneven charging occurs because electrical current flows more easily through the water-rich, low specific gravity electrolyte at the top than through the concentrated acid at the bottom, concentrating both current and heat in the upper plate regions and accelerating positive plate corrosion. Third, bottom plate sulfation is promoted as the concentrated acid at the bottom hinders effective charging of the lower plate regions, leading to irreversible sulfation. Finally, a false state of charge may be indicated, as the high acid concentration at the bottom artificially elevates the open-circuit voltage, making the battery appear more charged than it actually is.

L. Suggested Desulfation Strategies and Performance Optimization Recommendations for a Healthy Life of Lead-Acid Batteries During Peak Summer Seasons

Recovery from sulfation involves a combination of controlled charging and thermal techniques. First, the battery should undergo controlled overcharging at 14.8-16 V for 24-48 hours to gradually break down sulfate deposits. Second, elevating the battery temperature to 50-60 °C helps accelerate the dissolution of lead sulfate crystals. Finally, pulse charging techniques can be applied to mechanically disrupt the crystal structures, further aiding in the restoration of the battery's capacity. However, advanced sulfation often proves irreversible, necessitating battery replacement. Based on the electrochemical analysis and our empirical data, the following recommendations optimize lead-acid battery performance in solar applications. Effective battery longevity and performance rely on comprehensive management strategies encompassing temperature control, charge regulation, depth of discharge, humidity, maintenance, and system sizing.

1. Temperature Management involves maintaining battery temperatures between 15-25 °C through shading, ventilation, or insulated enclosures. Temperature-compensated charging should be implemented with a voltage adjustment of -3 to -5 mV/°C per cell, while direct sunlight exposure should be avoided. In hot climates, batteries should ideally be installed in cooler interior spaces to reduce thermal stress.
2. Charge Controller Settings are critical for optimal battery health. MPPT controllers should be configured for proper absorption voltage, typically 14.4-14.6 V at 25 °C for flooded batteries, with a float voltage set at 13.5-13.8 V to minimize overcharge stress. Temperature compensation should be enabled in controller settings, and periodic equalization cycles should be programmed every 2-4 weeks for flooded batteries to address stratification and sulfation.
3. Depth of Discharge (DoD) Management requires sizing battery banks to limit normal operation DoD to a maximum of 50%, while low-voltage disconnects should be set at 11.8-12.0 V to prevent deep discharge. For critical applications, a more conservative 30% DoD is recommended to maximize cycle life.
4. Humidity Control is essential due to the strong correlation between humidity and degradation. Batteries should be installed in ventilated, dry locations with 50-80% relative humidity, terminals treated with corrosion-inhibiting compounds, and dehumidification applied in humid climates. Regular inspection and cleaning of battery terminals are necessary to prevent corrosion-related failures.
5. Maintenance Protocols include monthly checks of electrolyte levels in flooded batteries, adding distilled water as needed, and quarterly specific gravity measurements to assess state of charge and detect stratification. Monthly equalization charges help combat stratification, and battery temperatures should be monitored during charging to detect thermal runaway.
6. System Sizing ensures consistent performance despite environmental and operational stresses. Oversizing solar arrays by 20-30% compensates for temperature-related degradation and ensures complete daily recharge. MPPT controllers should be rated 25-30% above maximum panel power to account for temperature coefficient variations. Additionally, monitoring systems tracking voltage, current, temperature, and humidity enable predictive maintenance and early detection of potential issues.

V. CONCLUSION

This research comprehensively demonstrates that incorporating real-time solar irradiance and key environmental parameters-including light intensity, temperature, and humidity-significantly enhances the predictive health assessment of lead-acid batteries in solar energy systems. The developed model, validated through empirical regression analysis and logistic classification, achieved high accuracy (96%) in classifying battery health under field conditions. Strong positive correlations between light intensity and both panel temperature and DC input voltage emphasize the dominant role of sunlight in charging efficiency, while the negative impact of humidity reinforces its status as a major degradation driver. Although model balance was challenged by limited degradation data, the framework provides critical quantitative insights and actionable strategies for system optimization. By explicitly integrating environmental and operational variables, this work advances beyond traditional battery monitoring approaches-enabling practical, robust, and interpretable predictive maintenance in distributed solar installations. The proposed methodology is scalable for real-world IoT deployment, offering a pathway to optimize charging cycles, extend battery life, and reduce premature failures in lead-acid storage systems.

VI. FUTURE SCOPE

Future extensions should focus on balancing datasets, exploring more advanced machine learning architectures, and broadening the approach to include other battery chemistries or operational regimes. Such improvements would further enhance early degradation detection and health prognostics, making predictive maintenance more robust and universally applicable across diverse solar energy storage systems.

ACKNOWLEDGEMENT

I express my sincere gratitude to Dr. Biswajit Mandal and Dr. Asim Halder for their valuable guidance and support in completing this research. I also thank my parents for their constant encouragement, my teachers for their dedication, and our Head of Department, Dr. Uday Majhi, for providing the opportunity to undertake this work.

Declaration of Conflicting Interests

The authors declare no potential conflicts of interest with respect to the research, authorship, and/or publication of this article.

Funding

The authors received no financial support for the research, authorship, and/or publication of this article.

Use of Artificial Intelligence (AI) - Assisted Technology for Manuscript Preparation

The authors confirm that no AI-assisted technologies were used in the preparation or writing of the manuscript, and no images were altered using AI.

ORCID

Swarnajit Bhattacharya http://orcid.org/0000-0002-8113-1816
Asim Halder http://orcid.org/0000-0002-4120-788X

REFERENCES

[1] D. E. O. Juanico et al., "Revitalizing lead-acid battery technology," *Frontiers in Batteries & Electrochemistry*, 2024.
[2] S. Jiang, "A review on the state of health estimation methods of lead-acid batteries," *Journal of Power Sources*, vol. 512, 2022.
[3] O. Bamisile et al., "The environmental factors affecting solar photovoltaic output," *Renewable and Sustainable Energy Reviews*, vol. 194, 2025.
[4] M. Tariq et al., "Analysis of the impact of irradiance, temperature and tilt on PV performance," *Solar Energy*, vol. 230, pp. 128-140, 2024.
[5] O. O. Apeh et al., "Modeling and experimental analysis of battery charge under varying environmental conditions," *Energy Reports*, vol. 7, pp. 1234-1245, 2021.
[6] D. Afonso et al., "Influence of long-term and short-term solar radiation on PV performance," *Energies*, vol. 18, no. 3, 2025.
[7] S. Bauknecht et al., "Electrochemical impedance spectroscopy as an analytical tool for the prediction of the dynamic charge acceptance of lead-acid batteries," *Batteries*, vol. 8, no. 2, 2022.
[8] P. Gasper et al., "Predicting battery capacity from impedance at varying states of charge," *NREL*, 2022.
[9] T. Murariu et al., "Time-dependent analysis of the state-of-health for lead-acid batteries," 2019.
[10] "Electrochemical Impedance Spectroscopy on Lead-Acid Cells," *RWTH Aachen Thesis*, 20xx.
[11] M. Mohsin et al., "A new lead-acid battery state-of-health evaluation method using EIS," *Journal of Energy Storage*, vol. 51, 2022.
[12] "Determination of SoH of Lead-Acid Batteries by EIS," *Academia.edu*, Methodology Review.
[13] G. R. Sylvestrin et al., "State of the art in electric batteries' state-of-health (SoH)," *Energies*, vol. 18, 2025.
[14] J. Wiselin and R. Rahiman, "Fixed frequency sliding mode-PI control for single phase unipolar inverters," *Asian Journal of Science and Applied Technology (AJSAT)*, vol. 2, no. 2, pp. 19-24, 2013.
[15] M. S. Nazim, "Artificial intelligence for estimating state of health and predictive maintenance of batteries," *ScienceDirect Review*, 2025.
[16] "Machine learning-based state of health prediction for battery systems," *ResearchGate*, 2025.
[17] R. Swarnkar et al., "A systematic literature review of state-of-health and predictive maintenance of batteries," *MDPI Transport*, 2023.
[18] J. Dong et al., "Data-driven model for predicting the current cycle count and SoH of lead-acid batteries," 2024.
[19] P. Senthil, "Effective monitoring of temperature and humidity in real-time wireless sensor method of processor and system architecture," *Asian Journal of Science and Applied Technology (AJSAT)*, vol. 7, no. 1, pp. 36-43, 2018.
[20] "What is battery degradation and how to prevent it," *Industry Technical Note*, 2025.
[21] H. Wen et al., "Extraction of health indicators from electrochemical impedance spectroscopy for lead-acid batteries," *ScienceDirect*, 2025.
[22] "Secure low-cost photovoltaic monitoring system based on LoRaWAN," *Springer*, 2024.
[23] "Automatic Solar Panel Monitoring System Using LoRa WAN," *IJMTST*, 2025.
[24] "Charge-controller optimization on lead-acid battery in solar PV systems," *ResearchGate*, 2022.
[25] "The effect of sun irradiance and temperature on the solar energy generation system," *ResearchGate*, 2025.
[26] "Real-time monitoring system for lead-acid battery health and performance using fuzzy logic and HIL simulator," *IJETT*, 2023.
[27] "Investigation of lead-acid battery water loss by in-situ EIS," *Electrochimica Acta*, 2024.
[28] T. Sohani, A. Sharma, and A. Sharmila Agnal, "MECABOT: A home security smartphone robot," *Asian Journal of Science and Applied Technology (AJSAT)*, vol. 7, no. 1, pp. 28-32, 2018.
[29] "Technological advances in lead-acid battery monitoring," *Industry Report*, 2025.
[30] S. Sharma and J. K. Sharma, "Entanglement measure based on matrix realignment," *Asian Journal of Science and Applied Technology (AJSAT)*, vol. 7, no. 1, pp. 17-19, 2018.